Mean field analysis of the $SO(3)$ lattice gauge theory at finite temperature

Srinath Cheluvaraja*
Tata Institute of Fundamental Research, Mumbai 400 005, India
(Received 8 October 1998; published 2 May 2000)

We study the finite temperature properties of the $SO(3)$ lattice gauge theory using mean field theory. The main result is the calculation of the effective action at finite temperature. The form of the effective action is used to explain the behavior of the adjoint Wilson line in numerical simulations. Numerical simulations of the $SO(3)$ lattice gauge theory show that the adjoint Wilson line has a very small value at low temperatures; at high temperatures, metastable states are observed in which the adjoint Wilson line takes positive or negative values. The effective action is able to explain the origin of these metastable states. A comparison of the effective actions of the $SU(2)$ and the $SO(3)$ lattice gauge theories explains their different behavior at high temperatures. Mean field theory also predicts a finite temperature phase transition in the $SO(3)$ lattice gauge theory.

PACS number(s): 12.38.Gc, 05.70.Fh, 11.15.Ha

Confining gauge theories are expected to pass over into a deconfining phase at high temperatures. The first explicit non-perturbative calculation [1] to show this was done in the strong coupling limit of lattice gauge theories (LGTs). Since then, there have been many studies of the finite temperature properties of LGTs. It is hoped that an understanding of their properties will shed some light on the high temperature phase of Yang-Mills theories. There have been numerous studies of the finite temperature properties of $SU(2)$ [2–4] and $SU(3)$ [5] LGTs. The basic observable that is studied in these systems is the Wilson-Polyakov line (henceforth called the Wilson line) which is defined as

$$L_f(x) = \mathrm{Tr}_f \exp\left(i \int_0^\beta A(x,x_4) dx_4 \right). \tag{1}$$

The subscript f indicates that the trace is taken in the fundamental representation of the group. The Wilson line has the physical interpretation of measuring the free energy $[F(x)]$ of a static quark in a heat bath at a temperature β^{-1}. This is made explicit by writing it in the form

$$\langle L_f(x) \rangle = \exp[-\beta F(x)]; \tag{2}$$

a non-zero value of the Wilson line implies that a static quark has a finite free energy whereas a zero-value implies that it has infinite free energy. The strong coupling analysis in [1] shows that the Wilson line remains zero at low temperatures and becomes non-zero at high temperatures [1], signalling a finite temperature confinement to deconfinement phase transition. This transition is also observed in numerical simulations. The action for the $SU(2)$ LGT is usually taken to be the Wilson action [6] and is given by

$$S = (\beta_f/2) \sum_{n\ \mu\nu} \mathrm{tr}_f\, U(n\ \mu\nu); \tag{3}$$

the subscript f indicates that the trace is taken in the fundamental representation of $SU(2)$. The variables $U(n\ \mu\nu)$ are the usual oriented plaquette variables:

$$U(n\ \mu\nu) = U(n\ \mu) U(n+\mu\ \nu) U^\dagger(n+\nu\mu) U^\dagger(n\ \nu); \tag{4}$$

the $U(n\ \mu)$s are the link variables which are elements of the group $SU(2)$. A finite temperature system (at a temperature β^{-1}) is set up by imposing periodic boundary conditions (with period β) in the Euclidean time direction. This results in an additional global $Z(2)$ symmetry that acts on the temporal link variables as follows:

$$U(n\ n_4) \to Z U(n\ n_4). \tag{5}$$

Z is an element of the center of the group $SU(2)$ and takes the values $+1$ or -1. Under the action of this symmetry transformation, the Wilson line transforms as

$$L(x) \to Z L(x). \tag{6}$$

It is evident that the high temperature phase (in which the Wilson line has a non-zero average value) breaks this global symmetry. As a result of this symmetry breaking, the high temperature phase of the $SU(2)$ LGT is doubly degenerate and the two states are related by a Z transformation. The two degenerate states have the same free energy because of this global symmetry. Numerical simulations observe these states as metastable states in which the Wilson line takes two different values which are related by a Z transformation. The role of the center symmetry was further emphasized in [3] where it was argued that the order of the transition to the high temperature phase could be understood in terms of the universality classes present in 3D spin models having this symmetry. These expectations have been borne out for the $SU(2)$ [4] and the $SU(3)$ [5] LGTs in which one observes a second order Ising like and a first order $Z(3)$ like phase transition respectively.

Another choice of an action, which is expected to lead to the same physics as the Wilson action, is the adjoint action that is given by

*Email address: srinath@theory.tifr.res.in

$$S=(\beta_a/3)\sum_{n\,\mu\nu}\mathrm{tr}_a\,U(n\,\mu\nu). \tag{7}$$

Here, the subscript a denotes that the trace is taken in the adjoint representation of $SU(2)$. The trace in the adjoint representation can be expressed in terms of the trace in the fundamental representation as

$$\mathrm{tr}_a U=\mathrm{tr}_f U^2-1. \tag{8}$$

From its definition, the adjoint action describes an $SO(3)$ LGT since the link variables $U(n\,\mu)$ and $-U(n\,\mu)$ have the same weight in the action. Unlike the $SU(2)$ LGT, the $SO(3)$ LGT has a bulk (zero temperature) transition at $\beta \approx 2.5$. This transition is understood in terms of the decondensation of $Z(2)$ monopoles [7]. An interesting and important question is whether the $SO(3)$ LGT has a deconfinement transition like the $SU(2)$ LGT. The universality of lattice gauge theory actions would require $SU(2)$ and $SO(3)$ LGTs to have the same continuum limit. We will show that our mean field analysis does predict a deconfinement transition in the $SO(3)$ LGT. In the $SO(3)$ LGT, the appropriate observable (though it is not an order parameter in the strict sense) to study deconfinement is the Wilson line in the adjoint representation [8]; this observable is defined as

$$L_a(x)=\mathrm{Tr}_a\exp\left(i\int_0^\beta A(x,x_4)dx_4\right). \tag{9}$$

The subscript a denotes the trace in the adjoint representation. The Wilson line in the fundamental representation is always zero in this model because of a local Z symmetry. This will be explicitly shown later. The adjoint Wilson line can also be interpreted as measuring the free energy of a static quark in the adjoint representation by writing it as

$$\langle L_a(x)\rangle=\exp[-F_a(x)]. \tag{10}$$

The Z symmetry acts trivially on this observable. A further generalization of the Wilson action is the mixed action LGT [9] that is defined as

$$S=(\beta_f/2)\sum_{n\,\mu\nu}\mathrm{tr}_f\,U(n\,\mu\nu)+(\beta_a/3)\sum_{n\,\mu\nu}\mathrm{tr}_a\,U(n\,\mu\nu). \tag{11}$$

The finite temperature properties of this model have been studied in [10].

The two Wilson lines can be expressed as a function of the gauge invariant variable θ as

$$L_f(x)=2\cos(\theta/2)\quad L_a(x)=1+2\cos(\theta); \tag{12}$$

θ is the phase of the eigenvalues of

$$P\exp\left(i\int_0^\beta A(x,x_4)dx_4\right). \tag{13}$$

The variable θ is gauge invariant and can be used to characterize the various phases of the system.

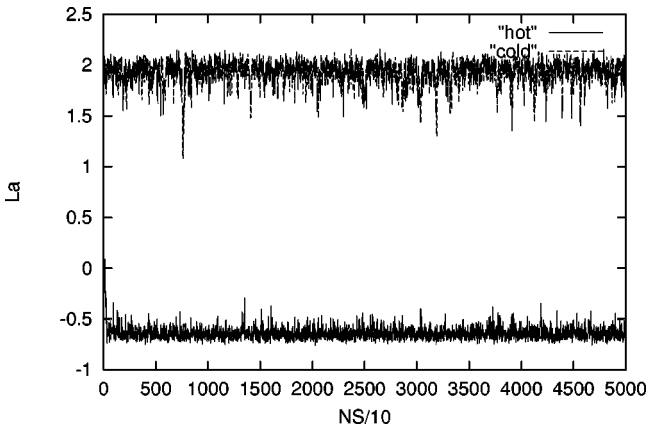

FIG. 1. The two metastable states for L_a. L_a is plotted as a function of (Monte Carlo sweeps)/10. The positive value is reached after a cold start and the negative value is reached after a hot start.

It is the purpose of the present paper to find the effective action, $V_{eff}(\theta)$, for the $SO(3)$ LGT at non-zero temperatures. The effective action is calculated in the mean field approximation. The effect of the fluctuations about the mean field solution is also considered and they are shown to be quite important at low temperatures. The effective action is also calculated for the $SU(2)$ LGT and the differences are pointed out with the $SO(3)$ LGT. We then make some comments on the mixed action LGT. Though a mean field analysis of the $SO(3)$ LGT is of interest in itself, the main motivation for our present analysis is to qualitatively understand some of the observations made in numerical simulations of the $SO(3)$ LGT. Numerical studies of the $SO(3)$ LGT [8] show that the adjoint Wilson line (AWL) remains close to zero at low temperatures and jumps to a non-zero value at high temperatures. Both the low and the high temperature behaviors of the adjoint Wilson line are quite puzzling. The small value of the AWL at low temperatures is surprising because a static source in the adjoint representation can always combine with a gluon and form a state with a finite free energy. More surprising, however, is the observation of two distinct metastable states for the AWL at high temperatures [8]. We explain later why we call these states metastable states. In numerical simulations, we find metastable states with the AWL taking a positive or negative value depending on the initial configuration of the Monte Carlo run. A hot start (random initial configuration) usually settles to a negative value whereas a cold start (ordered initial configuration) always settles to a positive value. This metastability is seen even at very high temperatures. Figure 1 is a typical run time history of the AWL for hot and cold starts in the high temperature phase. The values of other observables like the plaquette square and the $Z(2)$ monopole density (which is almost equal to zero) are almost the same in both these metastable states. All this appears very reminiscent of the metastable states (of the fundamental Wilson line) observed in the high temperature phase of the $SU(2)$ LGT in which two degenerate states related by a Z transformation are observed. Nonetheless, as there is no obvious symmetry in the $SO(3)$ LGT connecting the two observed metastable states, the presence of two exactly degenerate minima in the free en-

ergy would be quite remarkable. A measurement of the correlation function of the adjoint Wilson line indicated that the correlation lengths were the same in the L_a positive and L_a negative states [11]. The authors of [11] use this result to argue that the two states are physically equivalent. We will show the existence of these metastable states at high temperatures using mean field theory. The mean field analysis shows that there are minima in the effective action at positive and negative values of L_a. The difference in free energy density between these minima depends on two parameters, N_τ and β_a; N_τ is the temporal extent of the lattice (or the inverse temperature), and β_a is the coupling constant of the $SO(3)$ LGT. For a range of values of the parameters, N_τ and β_a, these minima are almost equal to each other. This may explain why both states are observed in numerical simulations. The mean field theory analysis can be done for the $SU(2)$ LGT as well, and the differences are pointed out with the case of the $SO(3)$ LGT. In particular, it is shown why the state in which the AWL takes a negative value is absent in the $SU(2)$ theory. Finally, we extend the mean field theory to the $SU(2)$ mixed action LGT. We conclude with a discussion of some theoretical issues connected with the adjoint Wilson line.

The usual approach of doing a mean field theory at nonzero temperature requires a strong coupling approximation as in [12]. There are other variants of this mean field theory which are all basically based on the idea of ignoring the effect of the spatial plaquettes [13]. Spatial plaquettes tend to deconfine the system; a deconfinement transition in the absence of spatial plaquettes will necessarily imply such a transition with them included. If one considers a reduced model with the spatial plaquettes discarded, the spatial links can be exactly integrated using a character expansion. This leads to an effective theory of Wilson lines in three dimensions. Before we present the details of this calculation, we would like to say that there is no qualitative change in the finite temperature properties of the system in this limit. The spatial degrees of freedom can be considered to be inert across the deconfinement transition, and the only role they play is to possibly shift the transition temperature. Symmetry properties are also not altered in anyway in this reduced model, and even the order of the phase transition, if there is any, should be unaffected by this simplification [this will be shown for the $SU(2)$ theory]. In this limit of the $SO(3)$ LGT, the L_a positive and L_a negative states are again observed in numerical simulations, just as in the full model, and they again display the same features as in the full model. The approximation of discarding the spatial plaquettes does not introduce anything extraneous into the finite temperature properties. Even the bulk properties of the system should remain unchanged in this approximation because ignoring the spatial plaquettes gives a zero weight to the $Z(2)$ monopoles which are known to drive the bulk transition [7] in the $SO(3)$ LGT. In the $SO(3)$ LGT, the $Z(2)$ monopoles anyway do not cost any energy because of the square term in the action. The main motivation for analyzing the reduced model is that an accurate mean field analysis can be made.

The reduced model is defined as

$$S=\sum_{p\in t}\chi(U); \tag{14}$$

the summation is only over the temporal plaquettes. $\chi(U)$ is a class function defined on the plaquette variables. We shall be concerned with three possible forms that this function can take. They are

$$\chi(U)=\frac{\beta_f}{2}\mathrm{tr}_f[U(p)]; \tag{15}$$

this is Wilson's action for the $SU(2)$ LGT. Then we will consider

$$\chi(U)=\frac{\beta_a}{3}\mathrm{tr}_a[U(p)]; \tag{16}$$

this is the adjoint action and describes an $SO(3)$ LGT. Finally, we will consider the mixed action,

$$\chi(U)=\frac{\beta_f}{2}\chi_f(U)+\frac{\beta_a}{3}\chi_a(U). \tag{17}$$

The character expansion of the exponential gives

$$Z=\int[DU]\prod_t\sum_j\tilde{\beta}_j\chi_j(U(p)). \tag{18}$$

The characters are given by the formula

$$\chi_j(\Omega)=\frac{\sin[(j+1/2)\theta]}{\sin(\theta/2)}. \tag{19}$$

Here Ω denotes some $SU(2)$ group element which is parametrized in the usual way as

$$\Omega=\cos(\theta/2)+i\vec{\sigma}\cdot\vec{n}\sin(\theta/2). \tag{20}$$

The $\tilde{\beta}_j$ can be calculated using the orthonormality property of the characters

$$\int[dU]\chi_r(U)\chi_s^*(U)=\delta_{rs}. \tag{21}$$

The character coefficients are given by

$$\tilde{\beta}_j=\int[dU]\exp[S(U)]\chi_j^*(U); \tag{22}$$

$S(U)$ can be the action for the $SU(2)$, $SO(3)$ or the mixed action LGT.

The spatial links can be integrated using the orthogonality relation

$$\int[DU]D^j_{m_1 n1}(U)D^k_{m_2 n_2}(U^\dagger)=\frac{1}{2j+1}\delta_{j,k}\delta_{n_1 m_2}\delta_{m_1 n_2}. \tag{23}$$

This leads to the effective 3D spin model with the partition function [with $\chi_j(\Omega(\vec{r}))$ acting as the spin degree of freedom]

$$Z=\int [d\Omega(\vec{r})]\prod_{\vec{r}'\vec{r}} \sum_j \left(\frac{\tilde{\beta}_j}{2j+1}\right)^{N_\tau} \chi_j(\Omega(\vec{r}))\chi_j(\Omega(\vec{r}')). \tag{24}$$

The effective action is

$$S_{eff}=-\sum_{\vec{r}'\vec{r}} \log \sum_j \left(\frac{\tilde{\beta}_j}{2j+1}\right)^{N_\tau} \chi_j(\Omega(\vec{r}))\chi_j(\Omega(\vec{r}')). \tag{25}$$

The partition function of this spin model can be written as

$$Z=\int [d\Omega(\vec{r})]\exp(-S_{eff}). \tag{26}$$

The measure is the $SU(2)$ Haar measure

$$d\Omega=\int_0^{4\pi}\frac{d\,\theta(\vec{r})}{4\pi}\{1-\cos[\,\theta(\vec{r})]\}. \tag{27}$$

So far, the analysis does not distinguish between the groups $SU(2)$ or $SO(3)$. The difference between them arises in the coefficients in the character expansion. In the $SU(2)$ LGT, all the character coefficients are in general non-zero and they are given by the formula

$$\tilde{\beta}_j=2(2j+1)I_{2j+1}(\beta_f)/\beta_f. \tag{28}$$

In the $SO(3)$ LGT, the $\tilde{\beta}_j$ are non-zero only for integer values of j and the coefficients are given by the formula

$$\tilde{\beta}_j=\exp(\beta_a/3)[I_j(2\beta_a/3)-I_{j+1}(2\beta_a/3)]. \tag{29}$$

For the mixed action LGT, all the character coefficients are non-zero but an expression similar to the one for $SU(2)$ and $SO(3)$ is not available, and the character coefficients have to be determined numerically. The properties of the character coefficients lead to an important difference between the effective spin models for the $SU(2)$ and the $SO(3)$ LGTs. Since the $SO(3)$ theory involves only the integer representations of $SU(2)$, the following relation is true for all the spins:

$$\chi_j(\theta(\vec{r})+2\pi)=\chi_j(\theta(\vec{r})). \tag{30}$$

This means that the transformation

$$\theta(\vec{r})\rightarrow\theta(\vec{r})+2\pi \tag{31}$$

is true at any single site. The above transformation is a local symmetry of the $SO(3)$ LGT. In the $SU(2)$ LGT, the following relation is true for the half-integer representations:

$$\chi_j(\theta(\vec{r})+2\pi)=-\chi_j(\theta(\vec{r})). \tag{32}$$

In the $SU(2)$ theory, the transformation in Eq. (31) is a symmetry only if it is performed simultaneously at every site. Thus the $SU(2)$ theory has only the following global symmetry:

$$\theta(\vec{r})\rightarrow\theta(\vec{r})+2\pi; \tag{33}$$

the $SO(3)$ theory has this symmetry as a local symmetry. Under these symmetry transformations, the fundamental and adjoint Wilson line transform as

$$L_f(\vec{r})\rightarrow -L_f(\vec{r})L_a(\vec{r})\rightarrow L_a(\vec{r}). \tag{34}$$

In the $SO(3)$ theory, this local symmetry (we will call it a local Z symmetry) ensures that the expectation value of the fundamental Wilson line is always zero.

We now look for a translationally invariant solution that minimizes the action in this model. This leads to the effective action

$$\frac{1}{N}S_{eff}(\theta)=-\log[1-\cos(\theta)]-3\log\left(\sum_j \frac{\tilde{\beta}_j}{2j+1}[\chi_j(\Omega)]^2\right). \tag{35}$$

The factor of 3 is present because we are dealing with a three dimensional spin model. The measure term has also been absorbed in the action. The partition function of the effective model is

$$Z=\int_0^{4\pi}[d\,\theta]\exp[-S_{eff}(\theta)]. \tag{36}$$

To get the effective action we have to deal with the infinite summation over j. Since the higher order terms in the character expansion are much smaller, the summation can be terminated at some large value of j. This approximation does not alter the results in any way as we have checked. We plot the effective action for the $SU(2)$ and $SO(3)$ LGTs as a function of θ. In the plot, the range of θ is restricted to vary from 0 to 2π since the other half gives no additional information. θ is the translationally invariant single site value of the phase of the Wilson line; it is a gauge invariant quantity. The shape of the effective action depends on the two parameters, N_τ and β_a or β_f. Depending on their values, the effective action develops one or more minima. The effective action for the $SU(2)$ theory for different values of β_f is shown in Fig. 2. At low temperatures, $V_{eff}(\theta)$ has the shape of a bowl with a very broad minimum at $\theta\approx\pi$. As the temperature increases, two minima start developing very close to the $\theta\approx\pi$ minimum and start receding away; at higher temperatures, these minima approach $\theta\approx 0$ and $\theta\approx 2\pi$. The two minima at high temperatures are the two states with a non-zero L_f which differ by a Z symmetry ($\theta\rightarrow 2\pi+\theta$) and they are the two phases with spontaneously broken Z symmetry. Both these states have the same value of L_a. These two minima in the effective action represent the deconfined phase of the $SU(2)$ LGT. The second order nature of the phase transition is also manifest from the evolution of the effective potential. This second order transition is seen in simulations

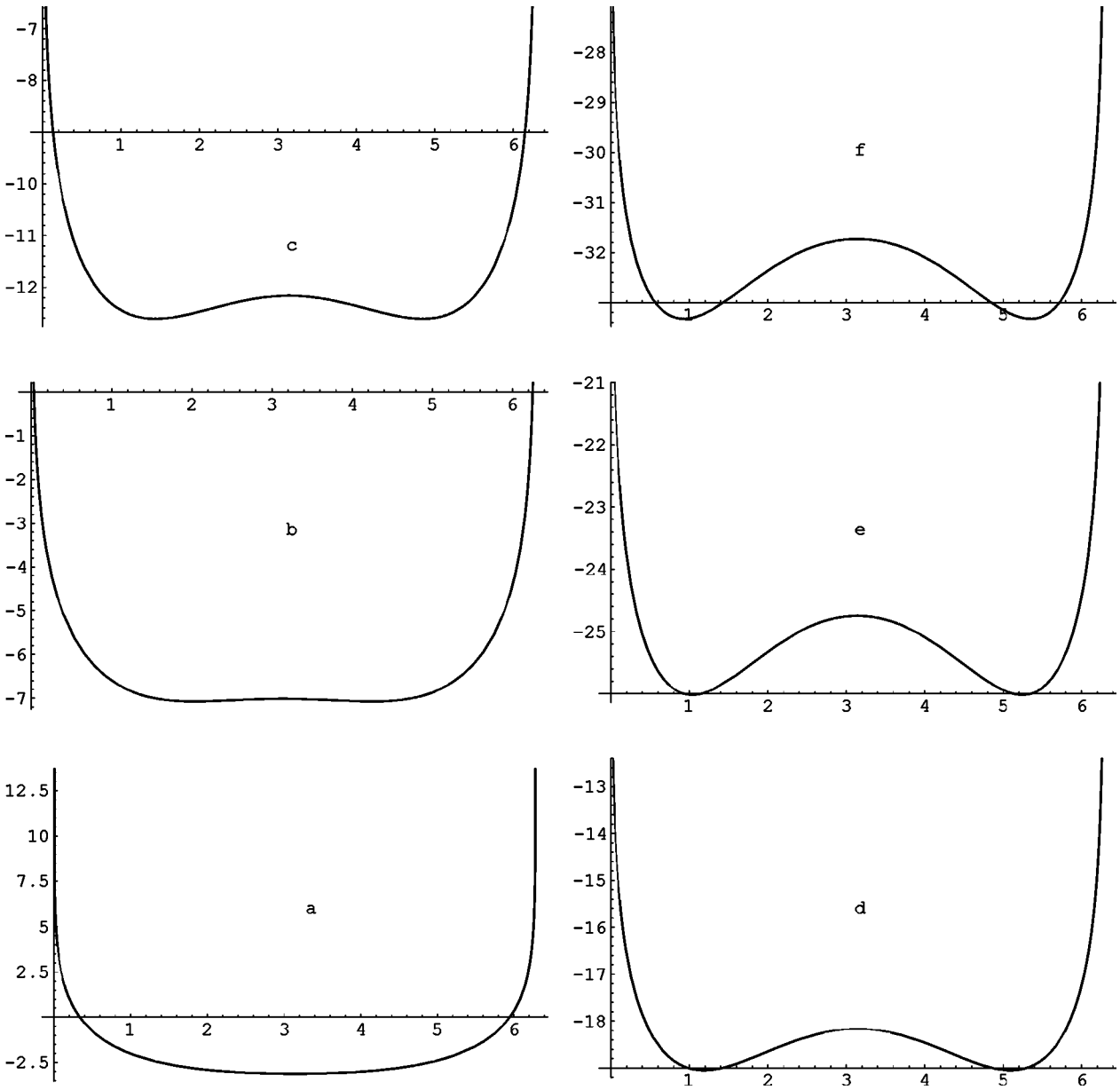

FIG. 2. The effective potential for the $SU(2)$ theory as a function of β_f with N_τ fixed to 3. The values of β_f for which the potential is shown are 1.5,2.5,3.5,4.5,5.5,6.5. In the figure these correspond to parts a,b,c,d,e,f respectively.

of the $SU(2)$ LGT, and is also in accordance with the universality arguments in [3]. We have demonstrated this result for the $SU(2)$ LGT, even though it is a well known one [12], simply because in our way of doing the mean field theory we use the phase of the eigenvalues of the Wilson line and not the trace of the Wilson line as is done in [12]. It also serves to show that a truncation of the spatial plaquettes does not change the finite temperature properties of the system. We now turn to the $SO(3)$ LGT theory which is our main interest. As we have mentioned before, the $SO(3)$ theory has a local Z symmetry and this is an important difference that we have to keep in mind. The effective action is shown in Fig. 3. At low temperatures, the effective action again develops the shape of a bowl with a very broad minimum at $\theta \approx \pi$. As the temperature is increased, the effective action evolves quite differently from the $SU(2)$ theory. The major difference from the $SU(2)$ theory is that the minimum at $\theta \approx \pi$ always remains a minimum. The broad minimum at $\theta \approx \pi$ gets sharper, and minima at $\theta \approx 0,2\pi$ start developing. The minimum at $\theta \approx \pi$ would correspond to a value of L_a equal to -1 and the minima at $\theta \approx 0,2\pi$ would correspond to a value of $+3$. The minima at $\theta \approx 0,2\pi$ have the same depth while the minimum at $\theta \approx \pi$ has a slightly different depth. The difference in the action between the two states depends on the values of N_τ and β_a. For the values of the parameters shown in the plot, the difference in depth of the minima at $\theta \approx 0,2\pi$ and the minimum at $\theta \approx \pi$ is small compared to the absolute value of these minima. For much larger values of β_a, the minima at $\theta \approx 0,2\pi$ sink below the minimum at $\theta \approx \pi$. Nevertheless, $\theta \approx \pi$ still remains a minimum, although it is only a local minimum. This evolution of the effective action signals a phase transition at large β_a across which the

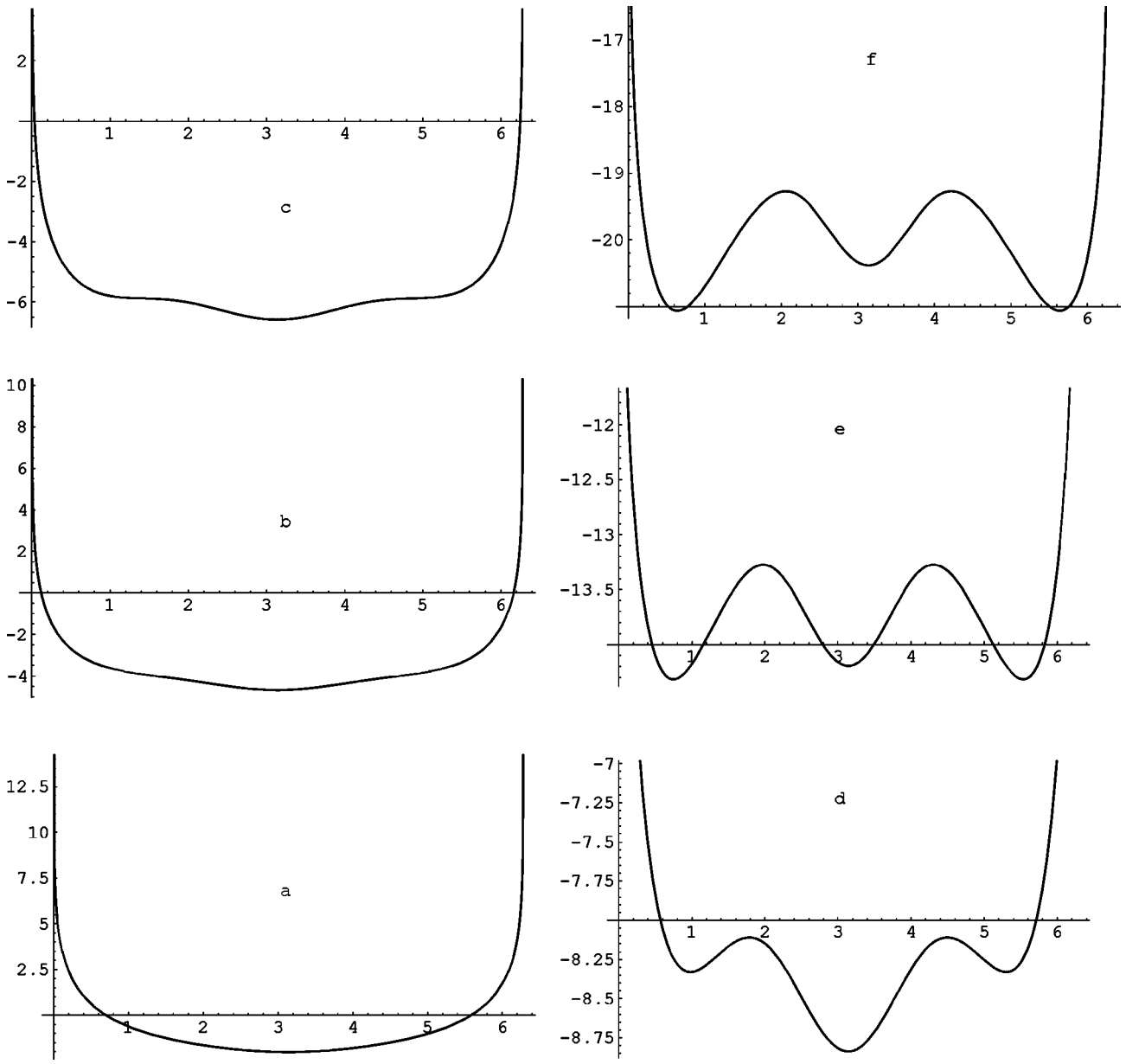

FIG. 3. The effective potential for the $SO(3)$ theory as a function of β_a with N_τ fixed to 3. The values of β_a for which the potential is shown are 1.5,2.5,3.0,3.5,4.5,5.5. In the figure these correspond to parts a,b,c,d,e,f respectively.

global minimum of the effective action shifts from $\theta \approx \pi$ to $\theta \approx 0,2\pi$. Though there are two minima in the effective action at the $\theta \approx 0,2\pi$, the local symmetry ensures that the average value of the fudamental Wilson line is always zero. The value of L_a is the same at $\theta \approx 0$ and $\theta \approx 2\pi$. Hence, the value of L_a in the minima at $\theta \approx 0,2\pi$ is the same as its value in the high temperature phase of the $SU(2)$ theory. We can then conclude that the global minima at high temperatures in the $SO(3)$ theory correspond to a deconfining phase just as in the $SU(2)$ theory, the only difference being that the adjoint Wilson line should be used to label the deconfining phase. As we have mentioned before, the average value of the fundamental Wilson line is zero because of the local symmetry. The minimum at $\theta \approx \pi$ is a new feature of the $SO(3)$ theory which is not present in the $SU(2)$ theory. We will now compare the results of our mean field calculation with the observations made in numerical simulations. To make this comparison, it is instructive to compare the distributions of the fundamental and adjoint Wilson lines (at a single site because the variable θ is the phase variable at a single site) observed in numerical simulations with the shape of the effective action. The distribution of L_a in the low and the high temperature states that are seen in simulations is shown in Fig. 4. At low temperatures, there is a bowl shaped minimum with a very broad peak at $\theta \approx \pi$. Thus the mean field solution predicts a value for L_a that is -1 at low temperatures. However, in simulations the expectation value of L_a is very small (almost close to zero) at low temperatures. The way to reconcile these two statements is to note that there are large fluctuations about the mean field solution at

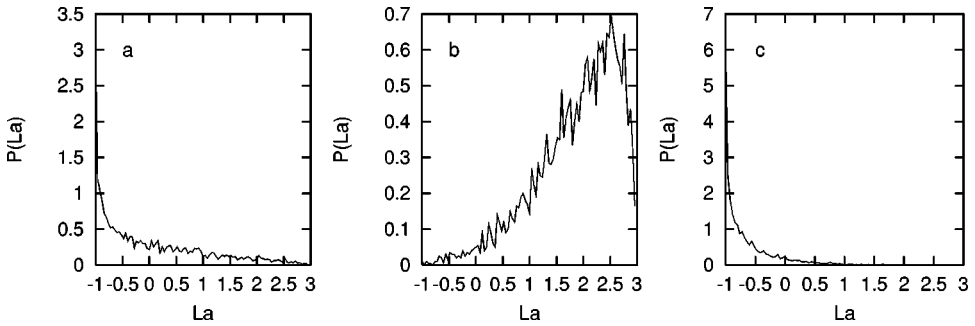

FIG. 4. The distribution of L_a in (a) the low temperature state, (b) the L_a positive state, and (c) the L_a negative state.

low temperatures. This is apparent from the flat shape of the effective potential at low temperatures. The second derivative of the effective potential at the minimum is quite small and this results in large fluctuations about the mean field solution. This is also seen from the distribution of L_a at a single lattice site, which is shown in Fig. 4a. This distribution has a very broad peak at $L_a \approx -1$ ($\theta \approx \pi$) but there are large fluctuations about this peak. A rough estimate of the fluctuations about the mean field solution can be made as follows. The effective potential can be approximated by retaining just the first two terms in the character expansion. This approximation is sufficient to reproduce the form of the effective potential in Fig. 3. The effective potential becomes

$$V(\theta(r)) = -\sum_r \log\{1-\cos[\theta(r)]\} - c\sum_{rr'} \{1+2\cos[\theta(r)]\} \times \{1+2\cos[\theta(r')]\}. \tag{37}$$

The constant c is $\tilde{\beta}_1/\tilde{\beta}_0$. We make the following expansion about the mean field solution:

$$V[\theta(r)] = V(\bar{\theta}) + (1/2)\sum_{rr'} \left.\frac{\partial^2 V}{\partial\theta(r)\,\theta(r')}\right|_{\bar{\theta}} \eta(r)\,\eta(r') + \cdots. \tag{38}$$

For the $\bar{\theta} = \pi$ state we note that

$$\left.\frac{\partial^2 V}{\partial^2\theta(r)\,\theta(r')}\right|_{\bar{\theta}} = 0 \tag{39}$$

and

$$\left.\frac{\partial^2 V}{\partial^2\theta(r)}\right|_{\bar{\theta}} = (1/2) + 12c. \tag{40}$$

This leaves only the following term in the expansion:

$$V(\theta(r)) = V(\bar{\theta}) + (V_1/2)\sum_r \eta^2(r) \tag{41}$$

where V_1 is given in Eq. (40). The partition function is given by

$$Z = \int d\bar{\theta} d\,\eta(r) \exp[-V(\bar{\theta})] \exp\left(-(V_1/2)\sum_r \eta^2(r)\right). \tag{42}$$

The corrected value of L_a in the presence of these fluctuations is given by

$$\langle L_a\rangle = (1/Z)\int d\bar{\theta} d\,\eta(r) \exp[-V(\bar{\theta})] \exp\left(\frac{-1}{2}V_1\sum_r \eta^2(r)\right) \times \{1+2\cos[\bar{\theta}+\eta(r)]\}. \tag{43}$$

Writing

$$2\cos[\bar{\theta}+\eta(r)] = [\exp i(\bar{\theta}+\eta(r)) + \text{c.c.}] \tag{44}$$

and doing a Gaussian integration we get the first correction to L_a as

$$\langle L_a\rangle = 1 + 2(-1)I, \tag{45}$$

where I is the following integral:

$$I = \frac{\int_{-2\pi}^{2\pi} d\,\eta \cos(\eta) \exp\left(\frac{-1}{2}V_1\eta^2\right)}{\int_{-2\pi}^{2\pi} d\,\eta \exp\left(\frac{-1}{2}V_1\eta^2\right)}. \tag{46}$$

V_1 is the second derivative of the effective potential at the minimum $\theta \approx \pi$. These fluctuations are large at low temperatures (which is the disordered phase) and are small at high temperatures (which is the ordered phase). Also, the above calculation is only for the leading order correction. There will be higher order corrections which will shift the value of L_a from the saddle point value even further. We have calculated this integral for some typical values in the low temperature phase and their effect is to shift the value of L_a (from the mean field value -1) by a large amount. At high temperatures, the corrections are smaller as the minima are more sharply peaked. This rough estimate of the fluctuations shows that fluctuations about the mean field solution (for the $\theta \approx \pi$ minimum) increase the value of L_a from the mean field value.

The distribution of L_a in the L_a positive state is peaked at a positive value of L_a. This can be compared with the two minima of the effective action at $\theta \approx 0$ and $\theta \approx 2\pi$. Both these minima have the same value (close to $+3$) of L_a. In

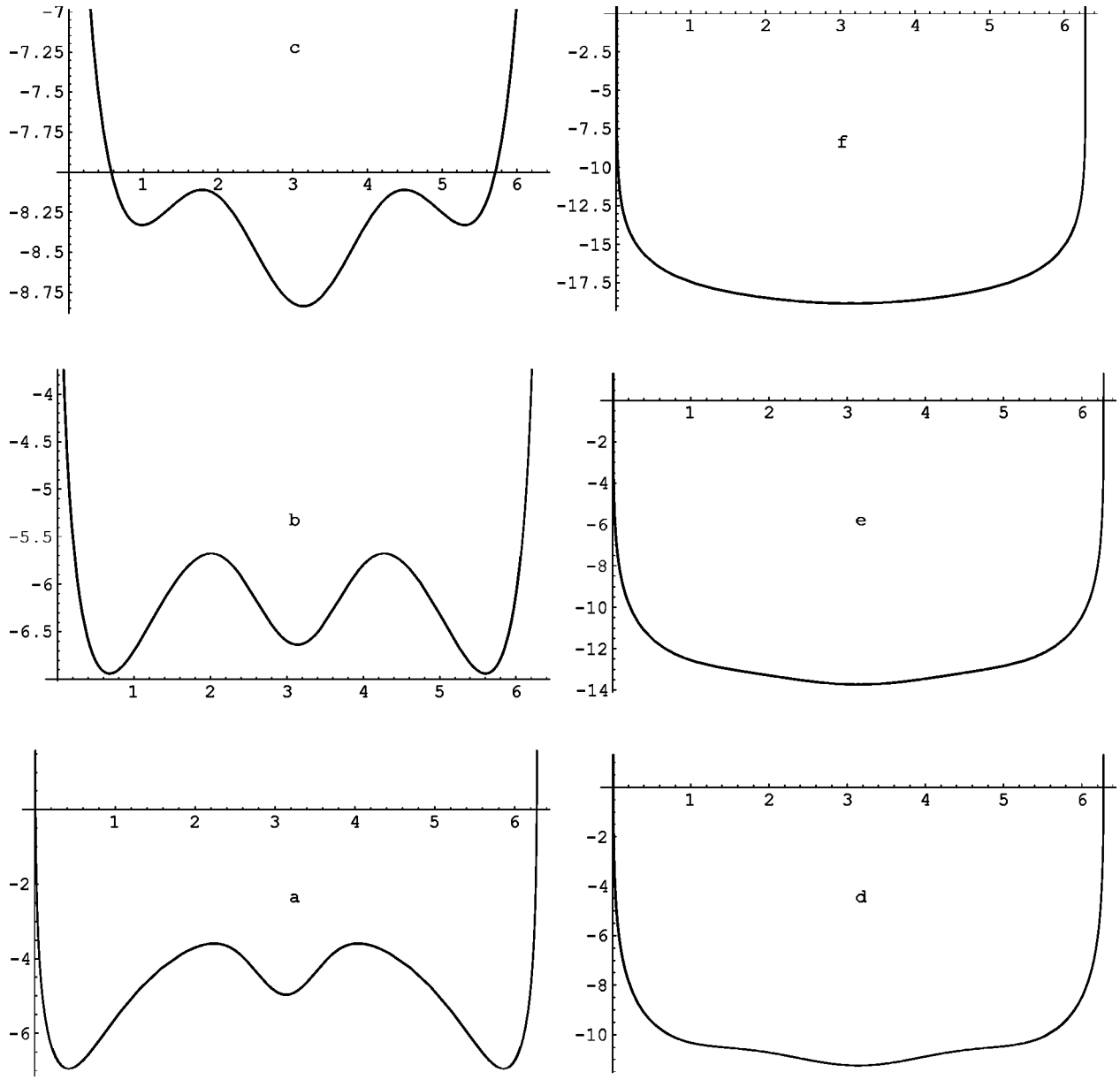

FIG. 5. The effective potential for the $SO(3)$ theory as a function of N_τ with a fixed β_a. The value of β_a is 3.5 and N_τ takes the values 1,2,3,4,5,7. In the figure these correspond to parts a,b,c,d,e,f respectively.

the L_a negative state, the effective action has a sharp minimum at $\theta \approx \pi$ and this can be compared with the distribution in Fig. 4c, which shows a sharp peak at $L_a = -1$ ($\theta \approx \pi$). As the minima are more sharply peaked at high temperatures, the corrections to the mean field value will be small. These observations show that the minima of the effective action along with the shape of the effective action near the minima (which represents the effect of fluctuations about the minima) can reproduce the structure of the high and low temperature states that are seen in numerical simulations. A notable aspect of the effective action is that the minima at $\theta \approx 0, 2\pi$ are exactly degenerate whereas the minimum at $\theta \approx \pi$ is slightly shifted from the other two. This is not very surprising because there is no symmetry between the $\theta \approx \pi$ and the $\theta \approx 0, 2\pi$ states which requires these states to be of the same depth. The minima at $\theta \approx 0, 2\pi$ are the same as those observed in the $SU(2)$ theory and correspond to the deconfining phase. The minimum at $\theta \approx \pi$ is at the same location as the minimum at low temperatures and is only more sharply peaked.

We have also studied the effective action at a fixed value of β_a and varied N_τ. Varying N_τ is equivalent to varying temperature at a fixed coupling. The purpose of this exercise is to see how the effective action evolves with temperature in the large β_a region. This evolution is shown for two values of β_a, 3.5 and 5.5. The evolution at these two couplings is shown in Fig. 5 and Fig. 6 respectively. At small N_τ (high temperatures), there are two global minima at $\theta \approx 0$ and $\theta \approx 2\pi$, and a local minimum at $\theta \approx \pi$; at large N_τ (low temperatures), there is only one bowl shaped minimum at $\theta \approx \pi$. This shows that as the temperature is raised at a fixed coupling, the global minimum of the effective action shifts

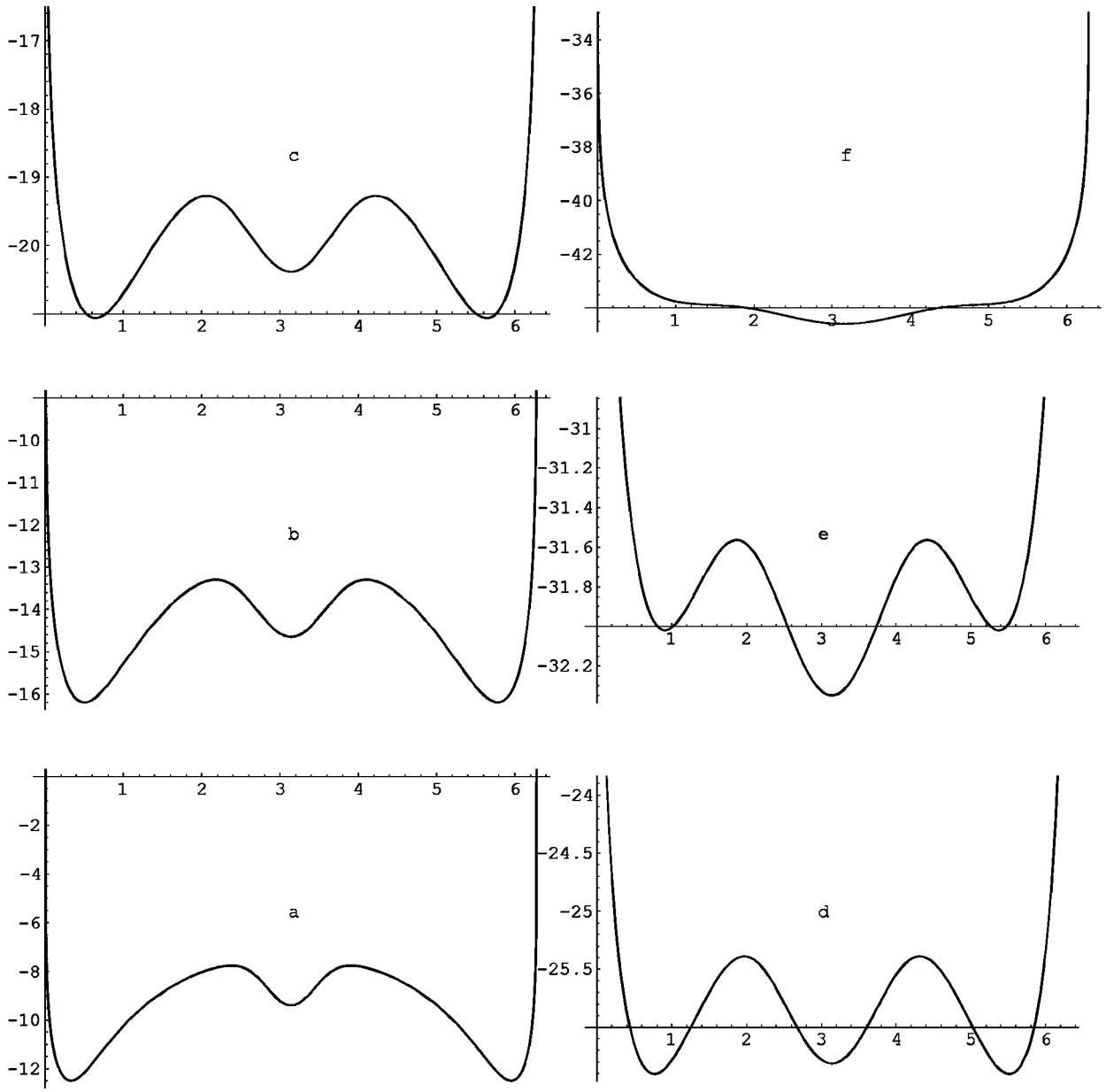

FIG. 6. The effective potential for the $SO(3)$ theory as a function of N_τ with a fixed β_a. The value of β_a is 5.5 and N_τ takes the values 1,2,3,4,5,7. In the figure these correspond to parts a,b,c,d,e,f respectively.

from $\theta \approx \pi$ to $\theta \approx 0,2\pi$. This again suggests that there is a finite temperature phase transition at a large coupling. The two evolutions also show that the transition to the deconfining phase takes place at $N_\tau = 3$ for $\beta_a = 3.5$ and at $N_\tau = 4$ for $\beta_a = 5.5$. Though the actual numbers predicted by the mean field calculation cannot be very accurate, the analysis does serve to demonstrate a definite trend as one increases β_a. As β_a increases, the transition temperature becomes lower (larger N_τ), and at least the direction in which β_a and N_τ are moving is not inconsistent with general expectations. Below we list some values of the critical coupling as a function of the lattice size:

N_τ	β_a^{cr}
2	3.2
3	4.4
5	6.3
7	8.2
9	10.1

We now wish to point out some features of the mean field theory which appear to be at variance with observations in numerical simulations. The evolution of the effective potential (see Fig. 3) as a function of temperature for a fixed value of N_τ shows that the minimum at $\theta \approx \pi$ continues to remain

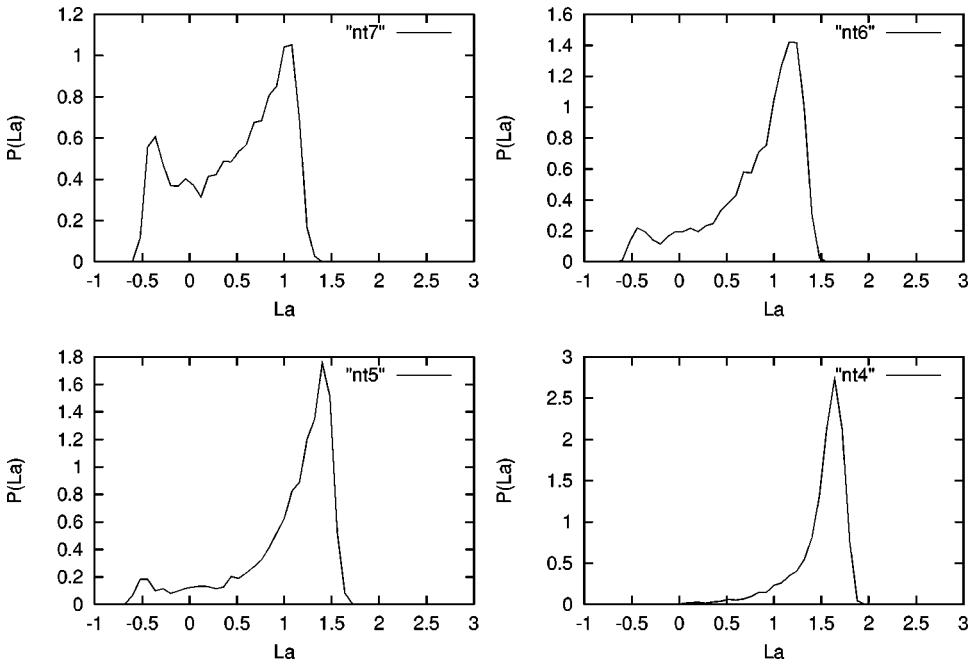

FIG. 7. The distribution of L_a as a function of N_τ at $\beta_a=3.5$. The spatial lattice size was fixed at $N_\sigma=7$ and the temporal lattice size is indicated in the figure key.

a minimum, although a sharpened one, even for reasonably large values of β_a. Though local minima start developing at $\theta\approx 0,2\pi$, the global minimum still remains at $\theta\approx\pi$. It is only at much larger temperatures that the minima at $\theta\approx 0,2\pi$ move below the minimum at $\theta\approx\pi$. In numerical simulations, a strong metastability in the value of L_a is observed at high temperatures. An ordered start always goes to the L_a positive state whereas a random start usually goes to the L_a negative state. Though the mean field theory shows that the free energy of these two states are never equal, both states are observed in simulations depending on the initial start of the Monte Carlo run. Another point is that even at large values of β_a, $\theta\approx\pi$ remains a local minimum; this may explain its appearance in simulations (with a hot start). A cold start, which begins at $\theta\approx 0,2\pi$, never settles to the L_a negative state. It is only the hot start which ever settles to the L_a negative state. This strong metastability in the values of the adjoint Wilson line persists even at very high temperatures. The other more striking feature predicted by the mean field theory, a phase transition from the $\theta\approx\pi$ state to the $\theta\approx 0,2\pi$ state, has not been directly observed in simulations, though there are strong indications that such a phase transition may be taking place [8]. An argument presented in [8] showed that the deconfinement transition in the $SO(3)$ LGT would require very large temporal lattices. Our studies of tunneling in [8] indicated a transition (as a function of temperature) from a double peak at $\theta\approx\pi,0,2\pi$ to a single peak at $\theta\approx 0,2\pi$. We present here one such plot of a tunneling study in Fig. 7. This figure shows the density of L_a as a function of N_τ on a $N_\sigma=7$ lattice at $\beta=3.5$. As N_τ is decreased, there is passage from the L_a negative region to the L_a positive region. This indicates the multiple peak structure in the effective action and also the passage from a double peak structure to a single peak structure at high temperatures. This should be compared with the evolution of the effective action shown in Fig. 5. The comparison is only meant to show a qualitative similarity in the two, and finer details (such as, the location of the passage from single peak to double peak) will certainly differ.

Next, we wish to mention a straightforward extension of the mean field theory to the $SU(2)$ mixed action LGT. The analysis proceeds as before and only the coefficients of the character expansion are different in this case. They have to be computed numerically using Eq. (22). For a fixed β_a and N_τ, the local minimum at $\theta\approx\pi$ disappears altogether for large β_f ($\beta_f\approx 1$), and the effective potential has the same form as in the $SU(2)$ LGT. This would imply that numerical simulations of the mixed action $SU(2)$ LGT should not observe the L_a negative state for large values of β_f. This feature is also confirmed in numerical simulations.

Finally, we would like to discuss some theoretical issues pertaining to the adjoint Wilson line which are quite different from the fundamental Wilson line. An appreciation of these differences is important for understanding the role of the adjoint Wilson line in the deconfinement transition. First, the adjoint Wilson line is not an order parameter in the strict sense and is always non-zero. Nevertheless, it can still show critical behavior across a phase transition. Another important difference between the fundamental and the adjoint Wilson line is that the average value of the adjoint Wilson line must always be non-negative. In the $SU(2)$ LGT, the average value of the fundamental Wilson line is always zero in a finite system because tunneling between the two Z related states always restores the symmetry. The adjoint Wilson line, on the other hand, is not constrained to be zero by any symmetry and is always non-zero, even on finite lattices. Also, the free energy interpretation in Eq. (10) presupposes that the average value of the adjoint Wilson line is a non-negative quantity. However, we are observing states of negative L_a in simulations. Though this negative value of the adjoint Wilson line is surprising, we note that in the large β_a region,

which is the region where we expect to make contact with Yang-Mills theory, the adjoint Wilson line is always positive.

From the above analysis it is evident that the mean field theory has had some success. For the first time we are able to explain the appearance of the L_a negative state and this state could not have been anticipated *a priori* from any considerations. The structure of the high and low temperature states observed in simulations is also explained. The mean field theory also predicts a phase transition in the large β_a region. In [8], various scenarios were suggested to reconcile the observations made in numerical simulations of the $SO(3)$ LGT with theoretical expectations. One of the scenarios suggested in [8] envisioned a phase transition from a bulk phase to a deconfining phase. The mean field theory has provided further evidence for this transition.

The author would like to acknowledge useful discussions with Rajiv Gavai and Saumen Datta. He would also like to thank J. Polonyi for an enlightening conversation, and for suggesting to him to perform a mean field analysis of the $SO(3)$ LGT.

Note added. In this paper we have not said much about the bulk, $Z(2)$ driven, transition in the $SO(3)$ LGT, but we have concentrated more on the behavior of the adjoint Wilson line. In our analysis, the effect of the bulk transition manifests itself in the sharpening of the minimum at $\theta \approx \pi$ and the appearance of minima at $\theta \approx 0,2\pi$ in the effective action at $\beta_a \approx 3$. In numerical simulations, the states with L_a negative and L_a positive are also observed immediately after the bulk transition.

Note 1. Regarding the L_a negative state we would like to point out that this negative value for L_a also implicitly appears in the mean field analysis of [12] for the $SU(2)$ LGT at low temperatures (since L_f is zero at low temperatures, L_a is negative). However, as we have shown earlier, the fluctuations about the mean field solution are important at low temperatures and produce a very small expectation value for L_a even in the $SU(2)$ gauge theory.

Note 2. As explained in the text, the neglect of the spatial plaquettes is not expected to change the finite temperature properties of the theory. It may be noted that the terms contributing to the effective potential of the $SU(2)$ theory as calculated in [12] do not include the spatial plaquettes, and yet these terms are sufficient to predict the finite temperature properties of the $SU(2)$ theory.

[1] A. Polyakov, Phys. Lett. **72B**, 477 (1978); L. Susskind, Phys. Rev. D **20**, 2610 (1979).
[2] J. Kuti, J. Polonyi, and K. Szlachanyi, Phys. Lett. **98B**, 199 (1980); L. McLerran and B. Svetitsky, *ibid.* **98B**, 195 (1980).
[3] L. Yaffe and B. Svetitsky, Nucl. Phys. **B210**[FS6], 423 (1982); Phys. Rev. D **26**, 963 (1982); B. Svetitsky, Phys. Rep. **132**, 1 (1986).
[4] R. Gavai and H. Satz, Phys. Lett. **145B**, 248 (1984); J. Engels, J. Jersak, K. Kanaya, E. Laermann, C. B. Lang, T. Neuhaus, and H. Satz, Nucl. Phys. **B280**, 577 (1987); J. Engels, J. Fingberg, and M. Weber, *ibid.* **B332**, 737 (1990); J. Engels, J. Fingberg, and D. Miller, *ibid.* **B387**, 501 (1992).
[5] K. Kajantie, C. Montonen, and E. Pietarinen, Z. Phys. C **9**, 253 (1981); T. Celik, J. Engels, and H. Satz, Phys. Lett. **125B**, 411 (1983); J. Kogut, H. Matsuoka, M. Stone, H. W. Wyld, S. Shenker, J. Shigemitsu, and D. K. Sinclair, Phys. Rev. Lett. **51**, 869 (1983); J. Kogut, J. Polonyi, H. W. Wyld, J. Shigemitsu, and D. K. Sinclair, Nucl. Phys. **B251**, 318 (1985).
[6] K. G. Wilson, Phys. Rev. D **10**, 2445 (1974).
[7] I. G. Halliday and A. Schwimmer, Phys. Lett. **101B**, 327 (1981); **102B**, 337 (1981); R. C. Brower, H. Levine, and D. Kessler, Nucl. Phys. **B205**[FS5], 77 (1982).
[8] S. Cheluvaraja and H. S. Sharatchandra, hep-lat/9611001.
[9] G. Bhanot and M. Creutz, Phys. Rev. D **24**, 3212 (1981).
[10] R. Gavai, M. Mathur, and M. Grady, Nucl. Phys. **B423**, 123 (1994); R. V. Gavai and M. Mathur, *ibid.* **B448**, 399 (1995).
[11] S. Datta and R. Gavai, Phys. Rev. D **57**, 6618 (1998).
[12] J. Polonyi and K. Szlachanyi, Phys. Lett. **110B**, 395 (1982).
[13] F. Green, Nucl. Phys. **B215**[FS7] , 383 (1983); F. Green and F. Karsch, *ibid.* **B238**, 297 (1984); J. Wheater and M. Gross, *ibid.* **B240** (1982).